Published as: *Cell*. 2014 January 30; 156(3): 482–494.

Extracellular architecture of the SYG-1/SYG-2 adhesion complex instructs synaptogenesis

Engin Özkan[1,2], **Poh Hui Chia**[3], **RuiqiRachel Wang**[4], **Natalia Goriatcheva**[1,2], **Dominika Borek**[5], **Zbyszek Otwinowski**[5], **Thomas Walz**[4,6], **Kang Shen**[2,3], and **K. Christopher Garcia**[1,2,*]

[1]Departments of Molecular and Cellular Physiology, and Structural Biology, School of Medicine,Stanford University

[2]Howard Hughes Medical Institute

[3]Department of Biology, Stanford University, Stanford, CA 94305, USA

[4]Department of Cell Biology, Harvard Medical School, Boston, MA 02115, USA

[5]Departments of Biochemistry, and Biophysics, University of Texas Southwestern Medical Center at Dallas, Dallas, TX 75390, USA.

[6]Howard Hughes Medical Institute, Harvard Medical School, Boston, MA 02115, USA

Abstract

SYG-1 and SYG-2 are multi-purpose cell adhesion molecules (CAMs) that have evolved across all major animal taxato participate indiverse physiological functions, ranging from synapse formation to formation of the kidney filtration barrier. In the crystal structures of several SYG-1 and SYG-2 orthologs and their complexes, we find thatSYG-1 orthologshomodimerizethrough a common, bi-specific interface thatsimilarlymediatesan unusual orthogonal docking geometry in theheterophilicSYG-1/SYG-2 complex.*C. elegans*SYG-1's specification of proper synapse formation *in vivo*closely correlates withthe heterophilic complex affinity, which appears to be tuned for optimal function. Furthermore, replacement of the interacting domains of SYG-1 and SYG-2 with those from CAM complexes that assume alternative docking geometries, or the introduction of segmental flexibility, compromised synaptic function. These results suggestthat SYGextracellular complexes do not simply act as "molecular velcro", but their distinct structural features are important in instructing synaptogenesis.

INTRODUCTION

Cellular adhesionhas enabled evolution of multicellular organisms and is a requirement formany different anatomical formations. It is regulated and mediated by interactions between cell surface receptors known as cell adhesion molecules (CAMs), which provide the physical strength of attachment, and also define the specificity of cells and subcellular

*Correspondence: kcgarcia@stanford.edu.

Accession numbers The coordinates and structure factors for the reported crystal structuresare deposited in the Protein Data Bank under PDB IDsXXXX, XXXX, XXXX, XXXX, XXXX, XXXX, XXXX, XXXX, XXXX, XXXX.

localizations that comprise the adhesive surfaces (Hynes and Zhao, 2000; Yamagata et al., 2003). Furthermore, these receptors can signal to initiate processes that lead to functional differentiation into one of many specific cellular adhesion structures, such as neuronal and immune synapses.However, the role of extracellular structure and ligand-receptor affinity in modulating the plethora of functions resulting from CAM engagement is not well understood. It is not clear if adhesion is structurally permissive and simply serves as 'molecular velcro,' or if the biophysical characteristics of the interactions are critical in triggering distinct functional outcomes.

Agroup of CAMs utilized in animals in many different adhesion structures is the family ofproteins homologous to *C. elegans* SYG-1 and SYG-2, which are immunoglobulin superfamily (IgSF) CAMs (Ig-CAMs) (Figure 1A)(Shen and Bargmann, 2003; Shen et al., 2004). These proteins not only specify synaptogenesisby mediating adhesion between guidepost vulval epithelial cells and the axon of the hermaphrodite-specific neurons (HSN) in *C. elegans* (Figure 1A), but also have adopted many other functions in arthropods and in vertebrates. SYG-1 and SYG-2 homologs are known to mediate muscle formation by specifying the fusion of muscle progenitor cells (myoblasts) in *Drosophila* and vertebrates(Dworak et al., 2001; Sohn et al., 2009; reviewed in Abmayr and Pavlath, 2012). They also control other processes in *Drosophila* that involve formation of proper cellular adhesions, such as the precise patterning of cells in the eye (Bao and Cagan, 2005; Ramos et al., 1993; Wolff and Ready, 1991), and sense organ spacing on the antennae (Venugopala Reddy et al., 1999),and are crucial in accurate formation of the optic chiasm(Boschert et al., 1990; Ramos et al., 1993; Schneider et al., 1995). Vertebrateorthologs of both proteins are strongly expressed in the nervous system, where new functions for the orthologous Neph proteins are emerging(Mizuhara et al., 2010; Serizawa et al., 2006; Völker et al., 2012). Intriguingly, orthologs of SYG-1 and SYG-2 have also been adopted in arthropods and vertebrates for building the hemolymph and blood filtration barriers, respectively, confirming that the two organsare evolutionarily related (Weavers et al., 2009).Mutations in the human SYG-2 ortholog,Nephrin, lead to a kidney disease called the congenital nephrotic syndrome of the Finnish type(Kestilä et al., 1998). SYG family proteins, therefore, constitute one of the most important and versatile CAMs in metazoans, involved in disparate cell adhesion functions ranging from synaptogenesis to blood filtration in kidney. Despite their prominence, the membrane-proximal downstream signaling events that result from extracellular engagement of SYGs and their orthologs are not entirely clear. Vertebrate Nephrinsare known to be phosphorylated, which leads to actin attachment (Jones et al., 2006; Verma et al., 2006), while F-actin was is recruited for SYG-specified synapse development in *C. elegans*(Chia et al., 2012). *C. elegans*SYG-1 also controls synapse elimination through directly inhibiting the ubiquitin ligase $SCF^{SEL\text{-}10}$(Ding et al., 2007). The most conserved intracellular feature of SYGs, a C-terminal PDZ domain-binding peptide, mediates interactions with juxtamembrane scaffolding proteins, such as ZO-1 and X11Lα (Huber et al., 2003; Vishnu et al., 2006).

Despite their importance in many aspects of animal physiology,the molecular basis of SYG-1 and SYG-2 interactions at cellular adhesion sites, and the role of structure in specifying function are not known.Here we ask if the structural and biophysical features of SYG extracellular complexes are important for conveying a proper functional outcome. Through a series of biochemical, biophysical and in vivo functional experiments,wefind that the extracellular affinity, docking geometry and rigidity of the SYG-1 and SYG-2 ectodomains play crucial roles, beyond simply adhesion, in specifying a functional synaptic architecture in *C. elegans*.

RESULTS

Interactions of SYG-1/SYG-2 complexes

The relative abilities of SYGs and their orthologs to form homo- versus heterophilic complexes reflect the acquisition of functional specification, and response to evolutionary pressures unique to each phylum. However, it is not clear which SYGs engage one another directly. Thus, we measured the homo- and hetero-typic interactions between a variety of SYG-1- and SYG-2-relatedproteins (Figure 1A), whichwerepreviously studied with cell aggregation assays and by co-immunoprecipitation, andhad yielded conflicting conclusions(Bao and Cagan, 2005; Dworak et al., 2001; Galletta et al., 2004; Gerke et al., 2003; Khoshnoodi et al., 2003; Schneider et al., 1995; Shelton et al., 2009; Wanner et al., 2011). Using isothermal titration calorimetry (ITC) and surface plasmon resonance (SPR),we showed that *C. elegans* SYG-1 and SYG-2 ectodomains form a complex with a dissociation constant (K_d) of ~0.6 μM(Figure S1, Table S1).We also expressed the first Immunoglobulin (Ig) domain of SYG-1 and the first four Ig domains of SYG-2 for crystallization,and these bound with similar affinity as the full-length ectodomains (Figure S1, Table S1).

These interactions are conserved across SYG orthologs, as we showed that the*Drosophila* homologs of SYG-1(Rst and Duf/Kirre) and of SYG-2(SNS and Hbs)all form hetero-complexes withaffinities between 1 to 4 μM (Figure S2, Table S1).Minimal complex-forming regions of the homologous *Drosophila* system were similarly mapped to within the first Ig domain of Rst or Duf, and the first four Ig domains of SNS or Hbs (Figure S2, Table S1). The similarity of the ectodomain interaction parameters among *Drosophila*and*C. elegans* SYGs suggests that this moderate affinity has been evolutionarily refined as optimal for SYG function.

Various SYG-1- and SYG-2-likeproteins have been previously reported to form homophilic complexes (Dworak et al., 2001; Gerke et al., 2003; Khoshnoodi et al., 2003; Schneider et al., 1995; Wanner et al., 2011); we did not detect high-affinity homophilic complexes for SYG-1, SYG-2 and their *Drosophila*orthologs. However, using a multivalentassay format to enhance avidity that we recently developed for detecting extracellular interactions(Özkan et al., 2013), we observed the reported Rst and Neph1 homophilic complexes(Gerke et al., 2003; Liu et al., 2003; Schneider et al., 1995), and a complexofRst and Duf(Özkan et al., 2013), all of which are SYG-1-like proteins.We showed with SPR that the Rsthomophilic complex was very low affinity(Figure S2I).We did not detect a *C. elegans* SYG-1 homophilic complex, or homophilic and heterophilic complexes between any SYG-2, in agreement with the previous reports on SYG interactions usingS2 cell aggregation assays for *C. elegans* and *Drosophila* SYGs(Shen et al., 2004; Dworak et al., 2001).We cannot, however, rule outvery weakcis-homophilic interactions for SYG-1 and SYG-2, as suggested by Shelton et al. (2009) and Wanner et al. (2011).

Structure of SYG-1: a conserved homodimeric interface

To acquire molecular insights into SYG-1 surfaces and the homophilic interactions of its orthologs, we first determined the crystal structure of the first domain (D1) and the first two domains (D1D2) of *C. elegans* SYG-1 (Figure 1B, Table S2).The D1 and D2 domainsboth adopt the canonicalimmunoglobulin fold with two β-sheets anda conserved disulfide bond linking the sheets through the B and F strands(Bork et al., 1994).The Ig domainsare co-linear, exhibiting extensive inter-domain contacts and segmental rigidity due to the absence of linker residues between the two domains(Figure S4A).We did not observe homodimers for any of these structures.

We then determined crystal structures of D1D2 of *Drosophila*Rst, the D1 of *Drosophila*Duf, and the D1D2 of mouse Neph1. In contrast to *C. elegans* SYG-1, we observe homodimeric structures forall of these SYG-1 orthologs mediated entirely by their D1 domains, consistent with our biochemical data (Figure 1C, Rst is shown). The homodimers are formed through interactions between the C'CFG sheets of the Ig domains (Figure 1C-D). The monomers create homodimers by docking against each other at nearly orthogonal anglesof 90° to 110° (Figure 1C), and this interaction geometryis conserved between the threeSYG-1-like homodimers. The Buried Surface Area of the homodimers is 1270 $Å^2$ ±50$Å^2$.These structures argue that arthropod and mammalian, but not nematode, SYG-1 orthologshomodimerizevia the observed common interface.

Three residues are prominent within thehomophilic interface: Q59, F65 and Q108 in Rst sequence numbering (Figure 1E). The two-fold symmetry axis relating the complex monomers bisects the two Q59 residues, whose contacts are mediated by two hydrogen bonds. F65 sits in a pocket, packing against the sidechain of Q108. To probe the energetic landscape of this interface, we used the Extracellular Interactome Assay (Özkan et al., 2013)to detect Rsthomodimerization (Figure 1E-F). We mutated Q59, F65, Q108, and R120, another F65-contacting residue. Alanine mutations of Q59 and F65 abolished the interaction, while Q108 and R120 diminished it significantly (Figure 1F). Q59 and Q108 are conserved in all SYG-1s, R120 is conserved in all non-nematode SYG-1s, and F65is part of a conserved hydrophobic patch (Figure 3D). Interestingly, all the mutations measured in the Interactome assaythat diminishedhomophilic interactions also diminished the heterophilic interactions (Figure 1F), indicating that these interaction interfaces overlap.

Structure of the SYG-1/SYG-2 heterophiliccomplex

To understand the molecular basis of the heterophilic interaction, we determined the crystal structure of the *C.elegans* SYG-1/SYG-2 complex containing the two N-terminal Ig domains of SYG-1 and the four N-terminal Igdomains of SYG-2 (Figure 2A-B). We solved the structure in several steps, using molecular replacement with our two-domain SYG-1 structure, *de novo* phasing of the fourth domain of SYG-2, followed by manual building of the remaining SYG-2 domainsaided by a SYG-2 D3D4 crystal structure.

In accord with our prior structure-function analysis(Chao and Shen, 2008) and in vitro mutational binding results (Figure 1F), the interaction between SYG-1 and SYG-2 is mediated entirely by theirN-terminalIg domains (D1). The D1s of SYG-1 and SYG-2 engage each other orthogonally, at an approximate 108° angle, resulting in an unusual L-like shape for the overall complex structure (Figure 2A-B). All the domains are co-linear with each molecule in an extended conformationdue to the lack of linker residues between the domains resulting in extensive inter-domain contacts (Figure S4A-C) and an overall rigidification of the molecules (Figure 2).

We interrogated the heterophilic interface by measuring the effects of mutations on SYG-1–SYG-2 binding affinity using SPR(Figures 2C-D and S3).SYG-1 residues centralto the heterophilicinterface and crucial for the interaction affinityare F60, Q105 and Q54, which are the equivalent residues that abolishedthe Rsthomophilic interaction when mutated (Figure 1F). At the center of the interface, SYG-1 Q54 interacts with SYG-2 Q53 in the same manner as seen for the Rst Q59 in thehomodimer. SYG-1 F60packs against SYG-2 Q105 within a pocket lined by SYG-2's F strand; these two residues are equivalent to Rst F65 and Q108, respectively. For SYG-2, the residue homologous to Rst F65 and SYG-1 F60 is a leucine (L61), which forms part of the C-C' loop of the Ig domain. This loop makes close van der Waals contacts to SYG-1 Q105.We also mutatedthe SYG-2 residues related to SYG-1/Rst residues Q54/Q59, F60/F65, Q105/Q108 and V116/R120; namely Q53, L61, Q105 and R115 (Figure S3B). Alanine mutagenesis of Q53, L61 and R115 caused an80- to

330-fold loss in affinity, and Ala mutation of Q105, which packs against the crucial F60 of SYG-1,essentially abolished the interaction. Thus, the energetic parsing of the interface reveals an asymmetry, whereby the SYG-1 F60 – SYG-2 Q105 pair is more energetically important for binding than its structurally symmetric SYG-2 L61 – SYG-1 Q105 pair.

The homophilic and heterophilic complexes of SYG-like proteins are mediated by bi-specific interfaces and common docking geometries

The amino acid contacts mediating the heterophilic SYG-1/SYG-2complex closely mimic those mediating thehomophilic complex interface, revealing a highly uncommon *dualspecificity* within one binding site.First, the heterocomplex of the SYG-1 and SYG-2 D1 domains are essentially superimposable with homodimeric complexes of Rst, Neph1 and Duf with an average of 1.1 ± 0.2 Åroot mean squared deviation (Figure 3A).Second, the SYG-1 residues participating in the homo- and heterophilicinterfacesare nearlyidentical, all belonging to the C'CFG faces of the Ig domains(Figures 3B-D). Third, loss of both homo- and heterophilic binding is observed when related residues in *C. elegans* SYG-1 and *Drosophila*Rst are mutated (Figures 1F, 3B, 3C).The interaction footprints of the homophilicbinding partner on Rst (Figure 3B) and the heterophilic binding partner on SYG-1 (Figure 3C) show similar surfaces and energetic contributions to their respective interactions, with the phenylalanine (F60) and the two glutamines (Q54 and Q105 in SYG-1) being most prominent. The patterns of conservation between SYG-1- and SYG-2-like proteins are a result of the 'pseudo'-symmetric nature of the heterophilic interactions, which also allows for the symmetric homophilic interaction.

Full ectodomain structures of SYG-1, SYG-2 and theircomplex

Despite being extended structures with multiple inter-domain 'joints', the similarity in the individualIgdomain positionsof the SYGs and their orthologs is remarkable (Figure 4A). This highlights a surprising rigidity that contrasts with the notion of 'beads on a string' for multi-domain CAM proteins with flexible domain boundaries.Therigidity of the SYGsis due to the lack of linker sequences between the Ig domains, forcing close-packed domain boundariesthat restrainflexibility(Figure S4A-C).Thisinflexibility could perhapscontribute to formation of arelatively rigid mesh comprised ofclustered SYG-1 and SYG-2 molecules at the site of a cell adhesion, such as the kidney filtration barrier. Rigidity would also more sensitively convey extracellular engagement to intracellular adaptor proteins. To gain a better appreciation of this issue, we studied the full-length free SYG-1 and SYG-2 ectodomains and the ectodomain heterodimer by negative-stain electron microscopy (EM) (Figure 4B-D). The molecules exhibited some regions of flexibility, potentially through very small inter-domain movements, resulting in parts of some of the molecules missing from most class averages, especially in the 10-domain SYG-2 (Figure S4D-F). Even small deviations in position would result in exclusion of these regions from averaged particles. However, some averages showed the entire five-domain SYG-1 ectodomain(Figure 4B) and up to eight domains of the SYG-2 ectodomain (Figure 4C). Averages mostly show extended conformations;we do not see 'bent' molecules (Figure S4D-F). We also observe 1:1 SYG-1/SYG-2 complexes with an orthogonal topology of interaction that is identical to that seen in the crystal structures (Figures 4D, S4F and S4G). Therefore, the EM images of the complex are consistent with extended structures lacking major inter-domain flexibility, and the orthogonal approach observed in our crystal structures.

SYG-1/SYG-2 affinity correlates with its synapse specificationfunction in vivo

The SYG-1/SYG-2 complex structure can serve as a guide for testing the functional consequences of disrupting this interaction in vivo. The interaction of SYG-1 with SYG-2 has been implicated in instructing the HSN neurons to form synapses specifically at the

vulva region(Shen and Bargmann, 2003; Shen et al., 2004). HSN forms *en passant* synapses onto vulval muscles that are clustered in a short and stereotyped segment (about 10 μm) of the HSN axon (Figure 5A, 5C). In *syg-1* mutants, synaptic vesicles fail to accumulate in the normal synaptic region and form ectopic synaptic clusters in the anterior axon (Figure 5B, 5D). If the SYG-1–SYG-2 interaction is controlling this event, we hypothesized that the interface we observed could be mutated to affect synaptogenesis at the vulva. We injected *syg-1*mutant animals with wild-type and SYG-2-binding mutants of*syg-1* under the control of the *unc-86* promoter, known to drive expression in the HSN neurons (Shen and Bargmann, 2003) (Figure 5E-H). As shown previously, we observed that wild-type SYG-1 completely rescued the synaptic vesicle clustering defects of *syg-1*mutants (Figure 5E), which we could measure either using quantitative fluorescence measurements of synaptic clusters on anterior sites on HSNL, or by a manual scoring of this phenotype in multiple independentlines (n≥50 animals for each line).The SYG-1 mutants selected covered a wide range of SYG-2 affinities, from 1.6-fold to 1,000-fold weaker than wild type. Mutant SYG-1 with mildly diminished affinity, such as D58A, only partially rescued the wild-type phenotype (Figure 5F), while mutations that practically abolished the interaction, such as F60A and the quadruple mutant, resulted in very little rescue of defects in *syg-1* mutants (Figure 5G, 5H). As expected, SYG-1 localization at HSN synapses is also dependent on SYG-1's affinity for SYG-2 (Figure S5). Overall, we observe a strong correlation between engineered affinities of the SYG-1–SYG-2 interaction with the rescue of the *syg-1*mutant defects (Figure 5I). Importantly, we find that even minor reductions in affinity (i.e. 1.6-fold) cause a synaptogenic defect, speaking to an endogenous interaction strength that is finely poised at a functional threshold. This suggests that the SYG-1/SYG-2 interface we have observed is the upstream controller of synaptogenesis of HSN neurons at the vulva, and that the strength of the SYG-1–SYG-2interaction is an important determinant for the efficiency of synaptogenesis.

SYG-1/SYG-2 interaction modules can be replaced with orthologous parts from *Drosophila* and mouse proteins in vivo

Based on the similarities between the heterophilic complex of *C. elegans*SYG-1/SYG-2 and the homophilic complexes of arthropod and mammalianhomologs,other hetero-complexes likely share the same structural features, including engagement geometry and interacting residues. Two studies have demonstrated thatthe full-length mouse SYG-1 and SYG-2 orthologs can partially rescue the synaptogenesis defects of *syg-1* and *syg-2* mutant worms(Neumann-Haefelin et al., 2010; Wanner et al., 2011). With new structural insight to guide us, we tested whether D1 domainsfrom the arthropod (Rst and SNS) and mammalian SYGs (Neph1 and Nephrin)can replace the D1sofSYG-1 and SYG-2 to rescue synapse defects in worms (Figure 6). For this purpose, we used *syg-1;syg-2*double mutant animals, and co-injected them with chimeric *syg-1* and chimeric *syg-2* under the *unc-86* and *egl-17* promoters, respectively. The *egl-17* promoter drives expression in the secondary vulva epithelial cells, and expression of *syg-2* with this promoter has been shown to reconstitute vulval synapses in a region slightly larger than the wild type (Figure 6A-D)(Shen et al., 2004).We observed that chimeras with*Drosophila*andmouse D1scan rescue the *syg-1;syg-2* phenotype (Figures 6E-F). However, the chimeric rescue was observed to be not as efficient as it was with wild type. We observed rescue in 79% of animals with *syg-1/syg-2*co-injections, but only in 38% and 23% of arthropod and mammalian chimeras, respectively (tabulated in Figure S6A). The partial penetrance is likely due to lower affinity on the part of the chimeras, which is five-fold weaker forRst and SNS (Figures S1, S2 and 7B).Similarly, SYG-1 Q54 mutant with an affinity sevenfold weaker than wild-type SYG-1 rescued *syg*-1 only 59% of animals, compared to 96% for wild type (Figure 5I, by phenotype penetrance). Nevertheless, the rescuesare statistically very significant ($p < 0.001$) compared to the controls of *syg-1* only and *syg-2* only injections (Figure S6A), and provide further evidence

that SYG-1–SYG-2molecular interactions are evolutionarily conserved across diverse taxa within metazoans.

Wanner et al. (2011) had observed that *C. elegans* SYG-1 could interact homophilically. We expressed *syg-1* with the *egl-17* promoter in a *syg-2* mutant background in an attempt to replace the SYG-1/SYG-2 complex with SYG-1 homodimers. We did not observe any rescue of the *syg-2* mutant phenotype (Figures S6C-D), which strengthens our view that nematode SYG-1 does not homodimerize, especially in a trans-cellular mode.

The observed docking geometry and rigidity of SYG-1 and SYG-2are necessary for SYG-1/SYG-2 complex function in vivo

We probed whether the orthogonaldocking geometry seen in the SYG-1 and SYG-2complexes is a necessary feature for synaptogenesis in vivo.For this, we inspectedpublished structures of alternative heterophilicIg-CAM complexes. When one of the domains of the alternative complexes are aligned with SYG-1 D1, as in Figure 7A, the orientations of the interaction partnersdisplay the spectrum of docking geometries Ig-CAMs adopt. The complex of the mouse Junction-Adhesion Molecule-like (JAML) protein with the mouse Coxsackie and Adenovirus Receptor (CAR) has the most similar interaction geometry to the SYG-1/SYG-2 complex(Verdino et al., 2010), with an 8 Å center-of-mass translation of CAR in relation to SYG-2, while the Sirpα/CD47 complex is the most structurally divergent(Hatherley et al., 2008), with CD47 displaced ~23 Å from the corresponding position of SYG-2 (Figure 7A). Both complexes have affinities within an order of magnitude of the affinity for the SYG-1/SYG-2 complex, and therefore we reasoned that their D1 domains might functionally substitute for the SYG-1 or SYG-2 D1 domains(Figure 7B) (Hatherley et al., 2008; Verdino et al., 2010).

We co-injected *syg-1;syg-2* animals with the mCAR-*syg-1* and mJAML-*syg-2*, and CD47-*syg-1* and Sirpα-*syg-2* chimeras. We find that CAR and JAML D1s can functionally replace the D1s for SYG-1 and SYG-2 in 25% of animals ($p > 0.001$) (Figure 7C). The rescue observed is similar to rescue by Rst/SNS and Neph1/Nephrinchimeras (Figure S6A), and this relatively efficient rescue occurs despite the nine-fold weaker affinity ofthe CAR-JAML interaction versus that of SYG-1–SYG-2. The CD47-Sirpα chimeras, however, did not rescue appreciably (8%) despite having an affinity nearly identical to the SYG-1–SYG-2 interaction (Figure 7B). Interestingly, we could recover function, as indicated by improved rescue (35%), when we replaced the wild-type CD47/Sirpα chimeras with an engineered variant of Sirpα, termed FD6, that binds to CD47 with~10,000-fold higher affinity than the wild-type protein(Weiskopf et al., 2013). Thus, it appears that the incompatible interaction geometry can be compensated, and overcome, to some degree, with sufficiently high affinity to compel an interaction. That the rescue is incomplete, despite such high affinity, supports the idea that the orthogonal architecture of the SYG-1/SYG-2 complex plays a specific ‘instructive’ role in *C. elegans* synaptogenesis, and that this adhesion event is not structurally permissive. This instructive role may be a direct result of the orthogonal architecture on signaling, or as an indirect consequence of changes in the cell-cell spacing distance with alternative receptor-ligand docking geometries.

To confirm that the chimeric proteins are expressed and targeted to the cell surface, we co-injected *syg-1syg-2*double mutant animals with chimeric SYG-1::GFP and SYG-2 pairs. All tested SYG-1 chimeras robustly localized to HSN axons, suggesting that they expressed and folded well (Figure 7D). Those SYG-1/SYG-2 chimeric pairs that rescued the synaptogenesis phenotype also displayed enrichment of SYG-1::GFP in the axonal segment contacting vulval cells, suggesting that the chimeric SYG-2 binding partners are also expressed and folded.

To test whether rigidity of the SYG ectodomains was important for function, we created SYG-1 and SYG-2 variants with ten-residue flexible linkersinserted at two domain boundaries downstream of the interacting domains (between D1-D2 for both, and between D2-D3 for SYG-1 and D4-D5 for SYG-2). When co-injected into *syg-1syg-2*double mutants, these proteins could not functionally replace rigid SYG-1 and SYG-2 completely, with rescue in 30% of animals (Figure 7C). Similar to the chimeras, we showed that the flexible SYG-1 localized to axons, indicating expression and correct folding. Intriguingly, this partial rescue was not accompanied by enrichmentatthe vulva (Figure 7D-6), raising the possibility that the rigid structure of the SYG extracellular complexes might contribute to the high-density packing of SYG-1 observed near the HSN vulval synapses.Overall, these results indicate that the rigid architecture of the SYG complex may also be required for formation of productive adhesion structures into an interaction plane, leading to synaptogenesis.

DISCUSSION

The broad question we address in this study is the role of structure and biophysical interaction parameters between an adhesive receptor-ligand pair in specifying function. It is unclear for most receptors whether extracellular engagement or ligand-induced multimerization alone is sufficient for function, or if the unique structural, and physical-chemical features of particular systems influence proper functional consequences. This issue is especially pertinent to CAMs, which generally cluster at adhesive sites, raising the question whether structure serves a more specific functional role than establishing a patch of‘molecular velcro.’

Roles for affinity, biophysical and structural properties in the SYG complexes

Here we interrogated this issue in a large family of multi-purpose Ig-CAMsthat mediate remarkably diverse functions such as synaptogenesis, myoblast fusion, axon guidance and formation of the kidney filtration barrier. We found thathomophilic and heterophiliccomplexes of SYG-1 and SYG-2 orthologs engage one anotherthrough an evolved dual specificity so as to have the capacity to form homophilic and heterophilic complexes.Furthermore, we demonstrated that the residues critically involved in the SYG-1–SYG-2 interfacemediate an interaction affinity that is ideal for proper synaptogenesis in *C. elegans*. In this way, the specific binding chemistry mediates an interaction affinity that has been fine-tuned for function. Remarkably, the interaction domains, D1s of SYG-1 and SYG-2, could be functionally replaced with orthologous domains from *Drosophila* and mouse, and even with domains from an unrelated Ig-CAM complex (JAM–CAR) as long as the complexes had asimilar orthogonal docking geometry to the SYG-1/SYG-2 complex. However, anotherIg-CAM complex with adifferent interaction geometry, CD47–Sirpα, failed to functionally rescue the *syg1;syg-2* phenotype.Furthermore, increasing the flexibility of the SYG ectodomains through the insertion of Gly-Ser linkers also lead to decreased rescue. Ourwork suggests that functional signaling initiated by SYG-like proteinsis critically linked to the architecture and physical chemistry of the extracellular interactions, and thus these parameters play ‘instructive’ roles in function.

Structural rigidity of adhesion molecules might have specific functional significance in diverse biological contexts. For example, the rigid tip-link adhesion complexes formed by cadherin molecules Pcdh15 and Pchd23 might be necessary to transform force into intracellular signaling(Sotomayor et al., 2012). Cadherins require calcium for rigidifying their ectodomains(Shapiro and Weis, 2009), which then protrude and are primed for trans interactions and cell-cell adhesion. The rigidity observed may also be a factor allowing close

packing of SYG complexes into a dense matrix within an interaction plane, facilitating downstream signaling through juxtamembrane recruitment of proteins and cytoskeleton.

Other cell surface receptor-ligand systems, such as cytokine or Tyrosine-kinase receptors for soluble growth factors, are activated through soluble ligand-induced oligomerization. CAMs, on the other hand, are comprised of interactions between two cell-associated membrane proteins that span an intercellular adhesive junction that, in most cases, is composed of tightly packed complexes (for example, Al-Amoudi et al., 2007). The surprising sensitivity of the SYG-1/SYG-2 complex geometry on preservation of itsspecific docking mode suggests a possibly great dependency on complex architecture within dense adhesive junctions to allow close packing of individual complexes to achieve not only the high density packing of receptors but also the highly regular subsynaptic spatial specifications. Interestingly, the prefusion complex during myoblast fusion, another SYG family protein mediated adhesion complex, was described as dense membrane plaques between apposed cells under EM, suggesting that this type of adhesion molecules effectively concentrate intracellular proteins.

Our results also link SYGs to another Ig-CAM family of proteinsthat exhibits homo- and heterophilic adhesion properties, the Nectins and Nectin-like proteins(Harrison et al., 2012). In this family of nine related proteins, heterophilic binding is consistently higher affinity than homophilic binding, similar toSYG-1- and SYG-2-like proteins. For Nectins, crystal structures have now demonstrated conserved modes of binding between homophilic and heterophilic interactions utilizing the same interface on the C'CFG face of the N-terminal immunoglobulin domains.

Structural Features of SYGs determine functional properties of their cellular adhesions

Our structural results are pertinent to many diverse SYG-mediated cell adhesions. As mentioned, the slit diaphragm of the kidney, which serves to filter blood, is constructed by SYG orthologs Neph1 and Nephrin. The thickness of the slit diaphragm has been measured to be ~40 Å(Haraldsson et al., 2008). Our complex model with elongated subunits and orthogonal interaction geometry based on our crystal structure and EM data spans 40 to 50 Å (Figure 7E), and is therefore consistent with the physiological distances measured for the slit diaphragm. Collectively, the newinsight we have gained into how the biophysical features of SYGs impact function will help to explain the functional architecture of the myriad of other known SYG-mediated cellular adhesions.

EXPERIMENTAL PROCEDURES

Protein Expression and Purification

All SYG-1, SYG-2 and orthologs, unless stated otherwise, were expressed using baculoviruses and High Five cells (Invitrogen) from *Trichoplusiani* by secretion into culture media as C-terminal hexahistidine-tagged proteins. SYG-2 D4 was expressed in High Five cells as an HRV 3C Protease-cleavable N-terminal hexahistidine- and Fc-fusion. Proteins were purified using Nickel-Nitrilotriacetic AcidAgarose resin (QIAGEN) and size exclusion chromatography in 10 mM HEPES pH 7.2, 150 mMNaCl. For selenomethionine labeling in bacteria, SYG-1 D1D2 was also refolded from inclusion bodies obtained by cytoplasmic expression in B834(DE3) cells (EMD Millipore).

Biophysical studies of proteininteractions

SPR experiments were performed with streptavidin (SA) chips using a Biacore T100 or 3000 (GE Healthcare). Proteins to be captured on SA chips were biotinylated at their C

termini using the *E. coli* biotin ligase BirA. Isothermal Titration Calorimetry experiments were done using a Microcal VP-ITC (GE Healthcare).

Crystallography of SYG-1, SYG-2 and their orthologs

SYG-1 was phased using multiple-wavelength anomalous diffraction methods with selenomethionine-labeled D1D2 crystals. Other SYG-1-like structures were solved by using SYG-1 D1D2 structure as molecular replacement models.SYG-2 D4 structure was solved using tantalum bromide cluster derivatives and the single-wavelength anomalous diffraction method. SYG-1/SYG-2 crystals could be grown using the N391C mutant of SYG-2, which removed an N-linked glycosylation site. The heterophilic complex was solved by a combination of molecular replacement with SYG-1 and SYG-2 D4,followed by manual rebuilding of all other domains, which was aided by homology modeling of with Modeller(Eswar et al., 2006) and our SYG-2 D3D4 structure.

All structural models were built and refined using Coot (Emsley et al., 2010)and Phenix.refine(Adams et al., 2010). Structure validation was performed by tools available within Coot and the PHENIX suit, mostly using Molprobity(Chen et al., 2010). For the mouse Neph1 D1-D2 structure, due to low resolution of the data, we refined the molecular replacement model by further creating homology models in Modeller(Eswar et al., 2006), followed by Dynamic Elastic Network refinement in CNS (Schröder et al., 2007).

Electron microscopy and image processing

Purified SYG-1, SYG-2 and cross-linked SYG-1/SYG-2 complex were prepared by conventional negative staining with 0.75% uranylformate(Ohi et al., 2004), and images were recorded on a Tecnai T12 microscope (FEI, Hillsboro,OR) at a nominal magnification of 42,000x with a defocus value of −1.5 μm. Particles were selected using BOXER, part of the EMAN2 software package (Tang et al., 2007), and processed using SPIDER (Frank et al., 1996).

C. elegansstrains—All worms strains were maintained at 20°C on OP50 *E. coli* seeded nematode growth medium plates. N2 Bristol stain worms were used as the wild-type reference and the following mutants were used: *syg-1(ky652)X, syg-2(ky673)X*. See the Extended Experimental Procedures for transgenic lines used in this study. Expression plasmids for transgenic worm lines were made using the pSM vector, a derivative of pPD49.26 (A. Fire). Plasmids were injected into animals at 1 ng/μl for the *unc-86* promoter and 15ng/μl for the *egl-17* promoter together with co-injection markers *Podr-1::gpf*or *Podr-1::dsred*at 20ng/μl.

Fluorescence quantificationand confocal imaging

All fluorescence images of HSNL synapses in L4 or young adults were taken with a 63x objective on a Zeiss Axioplan 2 Imaging System or a Plan-Apochromat 63x/1.4 objective on a Zeiss LSM710 confocal microscope. Total fluorescence intensity was determined using Image J software (NIH) by summing pixel intensity and the average fluorescence intensity was calculated for each group (n=10).

Supplementary Material

Refer to Web version on PubMed Central for supplementary material.

Acknowledgments

We would like to thank Suzanne Fischer and SeçilcanUyanıker for technical help, Lauren Ely for technical discussions, GeorgiosSkiniotis for preliminary EM imaging,Chia-Chi Ho for providing the amino acid sequence of Sirpα-FD6, andDemetAraç, MichaelE. Birnbaum and Fernando J. Bazanfor critical reading. This work is supported, in part, by 5 R01 NS048392 (K.S).K. Christopher Garcia, Kang Shen and Thomas Walz are investigators with the Howard Hughes Medical Institute.

References

Abmayr SM, Pavlath GK. Myoblast fusion: lessons from flies and mice. Development. 2012; 139:641–656. [PubMed: 22274696]

Adams PD, Afonine PV, Bunkóczi G, Chen VB, Davis IW, Echols N, Headd JJ, Hung L-W, Kapral GJ, Grosse-Kunstleve RW, et al. PHENIX: a comprehensive Python-based system for macromolecular structure solution. Acta Crystallogr. D Biol. Crystallogr. 2010; 66:213–221.

Al-Amoudi A, Déez DC, Betts MJ, Frangakis AS. The molecular architecture of cadherins in native epidermal desmosomes. Nature. 2007; 450:832–837. [PubMed: 18064004]

Bao S, Cagan R. Preferential adhesion mediated by Hibris and Roughest regulates morphogenesis and patterning in the Drosophila eye. Dev. Cell. 2005; 8:925–935. [PubMed: 15935781]

Bork P, Holm L, Sander C. The Immunoglobulin Fold: Structural Classification, Sequence Patterns and Common Core. J Mol Biol. 1994; 242:309–320. [PubMed: 7932691]

Boschert U, Ramos RG, Tix S, Technau GM, Fischbach KF. Genetic and developmental analysis of irreC, a genetic function required for optic chiasm formation in Drosophila. J. Neurogenet. 1990; 6:153–171. [PubMed: 2358965]

Chao DL, Shen K. Functional dissection of SYG-1 and SYG-2, cell adhesion molecules required for selective synaptogenesis in C. elegans. Mol. Cell. Neurosci. 2008; 39:248–257. [PubMed: 18675916]

Chen VB, Arendall WB 3rd, Headd JJ, Keedy DA, Immormino RM, Kapral GJ, Murray LW, Richardson JS, Richardson DC. MolProbity: all-atom structure validation for macromolecular crystallography. Acta Crystallogr. D Biol. Crystallogr. 2010; 66:12–21.

Chia PH, Patel MR, Shen K. NAB-1 instructs synapse assembly by linking adhesion molecules and F-actin to active zone proteins. Nat. Neurosci. 2012; 15:234–242. [PubMed: 22231427]

Ding M, Chao D, Wang G, Shen K. Spatial regulation of an E3 ubiquitin ligase directs selective synapse elimination. Science. 2007; 317:947–951. [PubMed: 17626846]

Dworak HA, Charles MA, Pellerano LB, Sink H. Characterization of Drosophila hibris, a gene related to human nephrin. Development. 2001; 128:4265–4276. [PubMed: 11684662]

Emsley P, Lohkamp B, Scott WG, Cowtan K. Features and development of Coot. Acta Crystallogr. D Biol. Crystallogr. 2010; 66:486–501.

Eswar, N.; Webb, B.; Marti-Renom, MA.; Madhusudhan, MS.; Eramian, D.; Shen, M-Y.; Pieper, U.; Sali, A. Comparative protein structure modeling using Modeller. Curr Protoc Bioinformatics Chapter 5, Unit 5.6. 2006.

Frank J, Radermacher M, Penczek P, Zhu J, Li Y, Ladjadj M, Leith A. SPIDER and WEB: processing and visualization of images in 3D electron microscopy and related fields. J. Struct. Biol. 1996; 116:190–199. [PubMed: 8742743]

Galletta BJ, Chakravarti M, Banerjee R, Abmayr SM. SNS: Adhesive properties, localization requirements and ectodomain dependence in S2 cells and embryonic myoblasts. Mech Dev. 2004; 121:1455–1468. [PubMed: 15511638]

Gerke P, Huber TB, Sellin L, Benzing T, Walz G. Homodimerization and heterodimerization of the glomerular podocyte proteins nephrin and NEPH1. J Am Soc Nephrol. 2003; 14:918–926. [PubMed: 12660326]

Haraldsson B, Nyström J, Deen WM. Properties of the glomerular barrier and mechanisms of proteinuria. Physiol. Rev. 2008; 88:451–487. [PubMed: 18391170]

Harrison OJ, Vendome J, Brasch J, Jin X, Hong S, Katsamba PS, Ahlsen G, Troyanovsky RB, Troyanovsky SM, Honig B, et al. Nectin ectodomain structures reveal a canonical adhesive interface. Nat. Struct. Mol. Biol. 2012

Hatherley D, Graham SC, Turner J, Harlos K, Stuart DI, Barclay AN. Paired receptor specificity explained by structures of signal regulatory proteins alone and complexed with CD47. Mol. Cell. 2008; 31:266–277. [PubMed: 18657508]

Huber TB, Schmidts M, Gerke P, Schermer B, Zahn A, Hartleben B, Sellin L, Walz G, Benzing T. The carboxyl terminus of Neph family members binds to the PDZ domain protein zonula occludens-1. J Biol Chem. 2003; 278:13417–13421. [PubMed: 12578837]

Hynes RO, Zhao Q. The evolution of cell adhesion. J. Cell Biol. 2000; 150:F89–96. [PubMed: 10908592]

Jones N, Blasutig IM, Eremina V, Ruston JM, Bladt F, Li H, Huang H, Larose L, Li SS-C, Takano T, et al. Nck adaptor proteins link nephrin to the actin cytoskeleton of kidney podocytes. Nature. 2006; 440:818–823. [PubMed: 16525419]

Kestilä M, Lenkkeri U, Männikkö M, Lamerdin J, McCready P, Putaala H, Ruotsalainen V, Morita T, Nissinen M, Herva R, et al. Positionally cloned gene for a novel glomerular protein--nephrin--is mutated in congenital nephrotic syndrome. Mol. Cell. 1998; 1:575–582. [PubMed: 9660941]

Khoshnoodi J, Sigmundsson K, Ofverstedt L-G, Skoglund U, Obrink B, Wartiovaara J, Tryggvason K. Nephrin promotes cell-cell adhesion through homophilic interactions. Am J Pathol. 2003; 163:2337–2346. [PubMed: 14633607]

Liu G, Kaw B, Kurfis J, Rahmanuddin S, Kanwar YS, Chugh SS. Neph1 and nephrin interaction in the slit diaphragm is an important determinant of glomerular permeability. J Clin Invest. 2003; 112:209–221. [PubMed: 12865409]

Mizuhara E, Minaki Y, Nakatani T, Kumai M, Inoue T, Muguruma K, Sasai Y, Ono Y. Purkinje cells originate from cerebellar ventricular zone progenitors positive for Neph3 and E-cadherin. Dev. Biol. 2010; 338:202–214. [PubMed: 20004188]

Neumann-Haefelin E, Kramer-Zucker A, Slanchev K, Hartleben B, Noutsou F, Martin K, Wanner N, Ritter A, Gödel M, Pagel P, et al. A model organism approach: defining the role of Neph proteins as regulators of neuron and kidney morphogenesis. Hum. Mol. Genet. 2010; 19:2347–2359. [PubMed: 20233749]

Ohi M, Li Y, Cheng Y, Walz T. Negative staining and image classification – powerful tools in modern electron microscopy. Biol. Proced. Online. 2004; 6:23–34. [PubMed: 15103397]

Özkan E, Carrillo RA, Eastman CL, Weiszmann R, Waghray D, Johnson KG, Zinn K, Celniker SE, Garcia KC. An Extracellular Interactome of Immunoglobulin and LRR Proteins Reveals Receptor-Ligand Networks. Cell. 2013; 154:228–239. [PubMed: 23827685]

Ramos RG, Igloi GL, Lichte B, Baumann U, Maier D, Schneider T, Brandstätter JH, Fröhlich A, Fischbach KF. The irregular chiasm C-roughest locus of Drosophila, which affects axonal projections and programmed cell death, encodes a novel immunoglobulin-like protein. Genes Dev. 1993; 7:2533–2547. [PubMed: 7503814]

Schneider T, Reiter C, Eule E, Bader B, Lichte B, Nie Z, Schimansky T, Ramos RG, Fischbach KF. Restricted expression of the irreC-rst protein is required for normal axonal projections of columnar visual neurons. Neuron. 1995; 15:259–271. [PubMed: 7646884]

Schröder GF, Brunger AT, Levitt M. Combining efficient conformational sampling with a deformable elastic network model facilitates structure refinement at low resolution. Structure. 2007; 15:1630–1641. [PubMed: 18073112]

Serizawa S, Miyamichi K, Takeuchi H, Yamagishi Y, Suzuki M, Sakano H. A neuronal identity code for the odorant receptor-specific and activity-dependent axon sorting. Cell. 2006; 127:1057–1069. [PubMed: 17129788]

Shapiro L, Weis WI. Structure and biochemistry of cadherins and catenins. Cold Spring Harb Perspect Biol. 2009; 1:a003053. [PubMed: 20066110]

Shelton C, Kocherlakota KS, Zhuang S, Abmayr SM. The immunoglobulin superfamily member Hbs functions redundantly with Sns in interactions between founder and fusion-competent myoblasts. Development. 2009; 136:1159–1168. [PubMed: 19270174]

Shen K, Bargmann CI. The immunoglobulin superfamily protein SYG-1 determines the location of specific synapses in C. elegans. Cell. 2003; 112:619–630. [PubMed: 12628183]

Shen K, Fetter RD, Bargmann CI. Synaptic specificity is generated by the synaptic guidepost protein SYG-2 and its receptor, SYG-1. Cell. 2004; 116:869–881. [PubMed: 15035988]

Sohn RL, Huang P, Kawahara G, Mitchell M, Guyon J, Kalluri R, Kunkel LM, Gussoni E. A role for nephrin, a renal protein, in vertebrate skeletal muscle cell fusion. Proc. Natl. Acad. Sci. U.S.A. 2009; 106:9274–9279. [PubMed: 19470472]

Sotomayor M, Weihofen WA, Gaudet R, Corey DP. Structure of a force-conveying cadherin bond essential for inner-ear mechanotransduction. Nature. 2012; 492:128–132. [PubMed: 23135401]

Tang G, Peng L, Baldwin PR, Mann DS, Jiang W, Rees I, Ludtke SJ. EMAN2: an extensible image processing suite for electron microscopy. J. Struct. Biol. 2007; 157:38–46. [PubMed: 16859925]

Venugopala Reddy G, Reiter C, Shanbhag S, Fischbach KF, Rodrigues V. Irregular chiasm-C-roughest, a member of the immunoglobulin superfamily, affects sense organ spacing on the Drosophila antenna by influencing the positioning of founder cells on the disc ectoderm. Dev. Genes Evol. 1999; 209:581–591. [PubMed: 10552299]

Verdino P, Witherden DA, Havran WL, Wilson IA. The molecular interaction of CAR and JAML recruits the central cell signal transducer PI3K. Science. 2010; 329:1210–1214. [PubMed: 20813955]

Verma R, Kovari I, Soofi A, Nihalani D, Patrie K, Holzman LB. Nephrin ectodomain engagement results in Src kinase activation, nephrin phosphorylation, Nck recruitment, and actin polymerization. J. Clin. Invest. 2006; 116:1346–1359. [PubMed: 16543952]

Vishnu S, Hertenstein A, Betschinger J, Knoblich JA, Gert de Couet H, Fischbach K-F. The adaptor protein X11Lalpha/Dmint1 interacts with the PDZ-binding domain of the cell recognition protein Rst in Drosophila. Dev. Biol. 2006; 289:296–307. [PubMed: 16380111]

Völker LA, Petry M, Abdelsabour-Khalaf M, Schweizer H, Yusuf F, Busch T, Schermer B, Benzing T, Brand-Saberi B, Kretz O, et al. Comparative analysis of Neph gene expression in mouse and chicken development. Histochem. Cell Biol. 2012; 137:355–366. [PubMed: 22205279]

Wanner N, Noutsou F, Baumeister R, Walz G, Huber TB, Neumann-Haefelin E. Functional and spatial analysis of C. elegans SYG-1 and SYG-2, orthologs of the Neph/nephrin cell adhesion module directing selective synaptogenesis. PLoS ONE. 2011; 6:e23598. [PubMed: 21858180]

Weavers H, Prieto-Sánchez S, Grawe F, Garcia-López A, Artero R, Wilsch-Bräuninger M, Ruiz-Gómez M, Skaer H, Denholm B. The insect nephrocyte is a podocyte-like cell with a filtration slit diaphragm. Nature. 2009; 457:322–326. [PubMed: 18971929]

Weiskopf K, Ring AM, Ho CCM, Volkmer J-P, Levin AM, Volkmer AK, Ozkan E, Fernhoff NB, van de Rijn M, Weissman IL, et al. Engineered SIRPα variants as immunotherapeutic adjuvants to anticancer antibodies. Science. 2013; 341:88–91. [PubMed: 23722425]

Wolff T, Ready DF. Cell death in normal and rough eye mutants of Drosophila. Development. 1991; 113:825–839. [PubMed: 1821853]

Yamagata M, Sanes JR, Weiner JA. Synaptic adhesion molecules. Curr Opin Cell Biol. 2003; 15:621–632. [PubMed: 14519398]

Highlight #1: Homophilic and heterophilic SYG-1/SYG-2 complexes share orthogonal binding geometries

Highlight #2: Homo- and heterophilic complexes are mediated by a shared binding interface.

Highlight #3: There is strong correlation between affinity of the complex and proper synaptogenesis

Highlight #4: Synaptogenesis is dependent on the approach geometry and rigidity of the SYG complex.

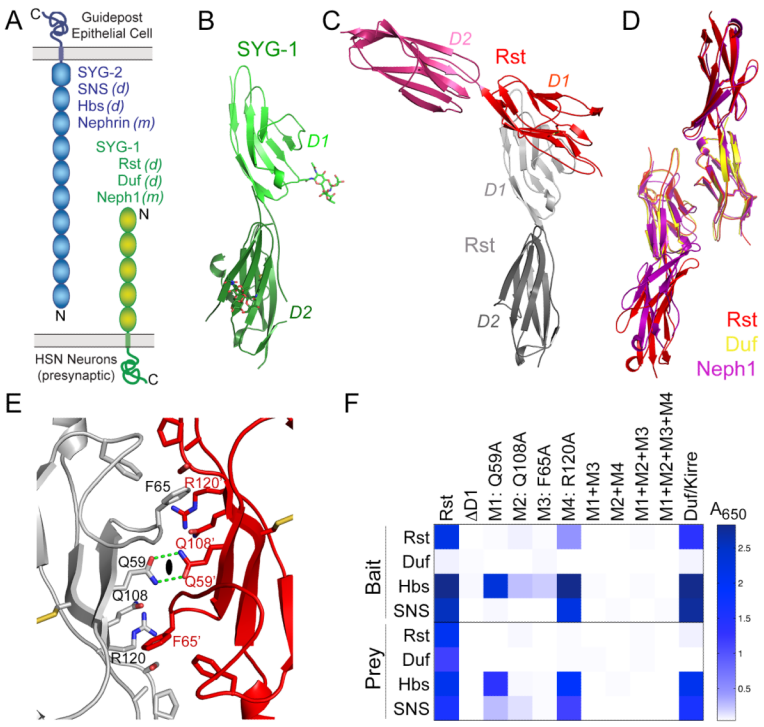

Figure 1. Structures of SYG-1 and homodimeric SYG-1-like complexes

A. Schematic representation of the domain structures of SYG-1 and SYG-2. All domains are of the Ig type except for the last domain of SYG-2, which is from the related FnIII domain family. Also noted are the *Drosophila melanogaster(d)* and mammalian *(m)*orthologs.

B. The crystal structure of *C. elegans* SYG-1 domains 1 and 2 (D1 and D2), in light and dark green, respectively. N-linked glycosylation is depicted in sticks representation.

C. The homodimeric structure of Rst D1-D2, demonstrating the near-orthogonal approach of the monomers.

D. Overlay of structures solved of *Drosophila* and mouse SYG-1-like proteins. The close match between the homodimeric structures of Rst (red and orange), Duf/Kirre (yellow), and Neph1 (purple) demonstrate that the crystallographicallyobserved homodimers are conserved and physiological.

E. Close-up of the symmetrical Rsthomodimer interface. The 2-fold sign (closed oval) represents the homodimersymmetry axis. The prime sign is added to residue labels for the Rstmonomer displayed in red.

F.The Extracellular Interactome Assay (Özkan et al., 2013) for wild-type Rst and mutants against wild-type Rst, Duf, Hbs, and SNS. The assay was performed in both orientations, as wild-type Rst, Duf, Hbs and SNS as bait (above), and as prey (below). The scale, colored as white to blue, represents absorbance values at 650 nm as the assay outcome. See also Figure S1 and Table S1.

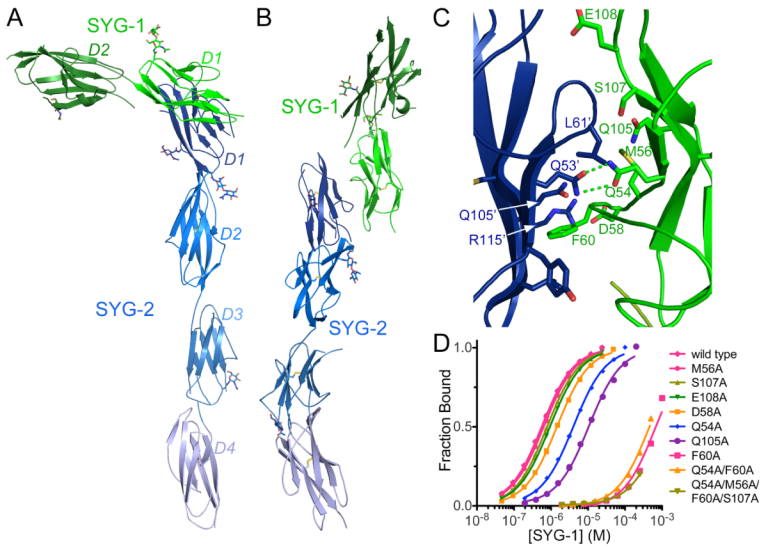

Figure 2. Structure of the SYG-1/SYG-2 heterophilic complex

A-B. Two different views of the crystal structure of the complex of SYG-1 (green) and SYG-2 (blue), in which individual Igdomains are labeled in different shades of the respective colors. N-linked glycosylation is represented as sticks. See Table S2 for crystallography statistics.

C. Close-up view of the SYG-1/SYG-2 heterophilic interface. Prime signedresidue labels belong to SYG-2 residues.

D. Bindingisotherms for the interactions of wild type and mutantSYG-1 with SYG-2 as measured by SPR. See Figure S2 for SPR data for *Drosophila* SYGs.

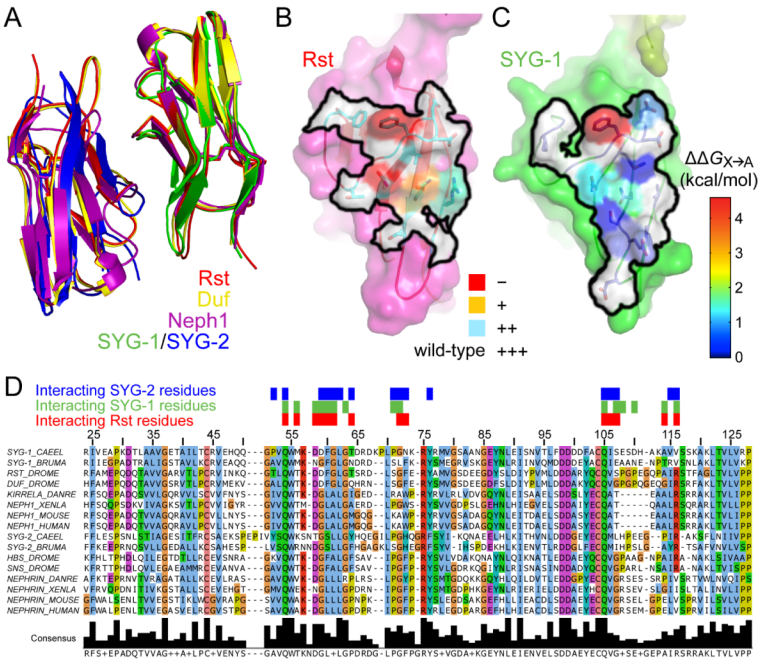

Figure 3. Comparison of homophilic and heterophilicSYG-likecomplexes

A.D1s in four complex structures are overlayed to demonstrate the conservation between the homophilic and heterophilic binding modes.

B. Surface representation of the interaction footprint (black outline) in the homodimericRst complex. The outline includes residues within 4 Å of the other Rst monomer.Cyan, orange and red represent increasing loss of binding as observed in Figure 1F upon mutagenesis of the labeled residues to alanine.

C. Surface representation of the interaction footprint (black outline) of the SYG-1/SYG-2 complex on SYG-1. Within the black outline, blue to red coloring indicates increased loss of binding upon mutagenesis, as measured in Figure 2D, but converted to change in free energy.

D. Sequence alignment of first domains (D1) of SYG-1-like and SYG-2-like proteins from the nematodes *C. elegans* and *Brugiamalayi*, fruit fly (*D. melanogaster*), zebrafish(*D. rerio*), frog (*X. laevis*), mouse and human. The sequence numbering is for the *C. elegans* SYG-1. The red, green and blue boxes above the sequences represent residues of Rst, *C. elegans* SYG-1 and *C. elegans* SYG-2 that are within 4 Å of their interaction partners. See also Figure S3.

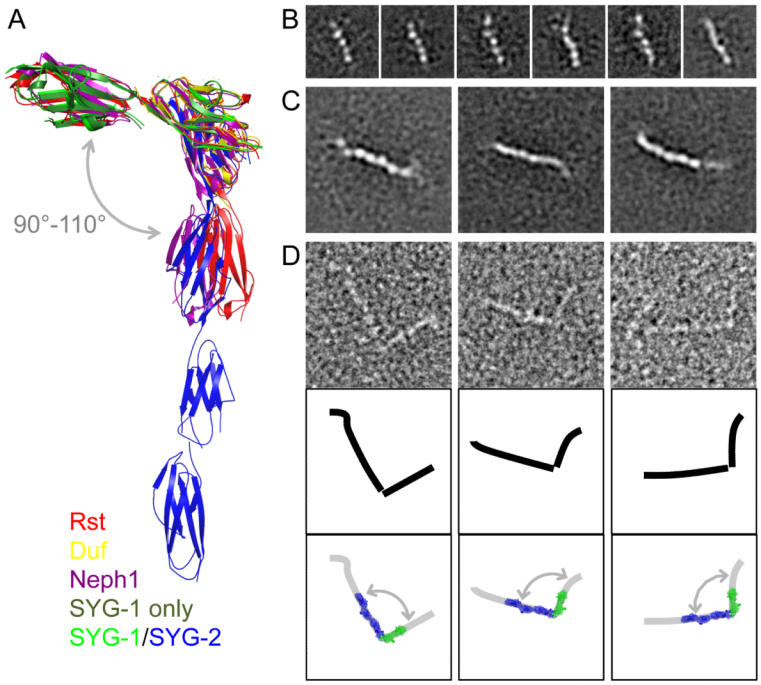

Figure 4. SYG-1 and SYG-2 exist in extended conformations

A. Overlay of five SYG-1 andSYG-1/SYG-2-like complexes solved. The overlay demonstrates that there are only minor movements ("swings") between the domains. **B-D.**Electron microscopy of negatively stained SYG-1 and SYG-2. The side length of the individual panels is 25 nm in (B) and 50 nm in (C) and (D).

B.Selected class averages of the five-domain ectodomain of Syg-1. All class averages are shown in Figure S4A.

C.Selected class averages of the ectodomain of SYG-2. All class averages are shown in Figure S4B.

D. Raw particle images of SYG-1/SYG-2 complexes (top), schematic drawings (middle), and the schematic drawings overlaid with the crystal structure of SYG-1-D1-D2/SYG-2-D1-D4 (bottom). See also Figure S4C-G.

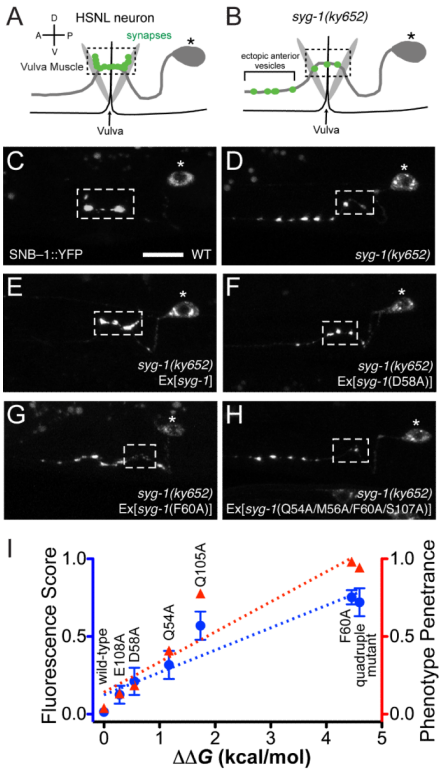

Figure 5. Affinity of the SYG-1/SYG-2 complex correlates with synaptic vesicle defects at the HSNL neuron

A-B. Schematic representation of HSNL synapses at the vulva in wild-type (A) and *syg-1* worms (B). The dashed box shows wild-type synaptic region.

C. Wild-type worms make synapses only at the primary synaptic region at the vulva (within the box).

D, E.*syg-1* animals show ectopic anterior synaptic vesicles. This is rescued when wild-type *syg-1* is expressed in HSN.

F. SYG-1 D58A, a mutant with moderate loss of SYG-1 affinity, partially rescues the *syg-1* mutant synaptic vesicle phenotype.

G, H. SYG-1 F60A and the quadruple mutant, neither of which have appreciable affinity for SYG-2, do not rescue the *syg-1* phenotype.

I. Correlation between affinities of SYG-1 mutants and the *syg-1* phenotype. The *syg-1* synaptic vesicle phenotype has been measured as both a fluorescence score, a quantitation of ectopic anterior vesicles over ~10 animals, and as a phenotype penetrance score, an all (1), partial (0.5), or none (0) scoring of the synaptic vesicle phenotype in >100 animals. These are compared against loss of binding energy upon the indicated mutations on SYG-1, and show very high correlations to the fluorescence score (R^2 = 0.89, blue dashed line) and to the phenotype penetrance (R^2 = 0.88, red dashed line). See Figure S5 for SYG-1 clustering at the vulva.

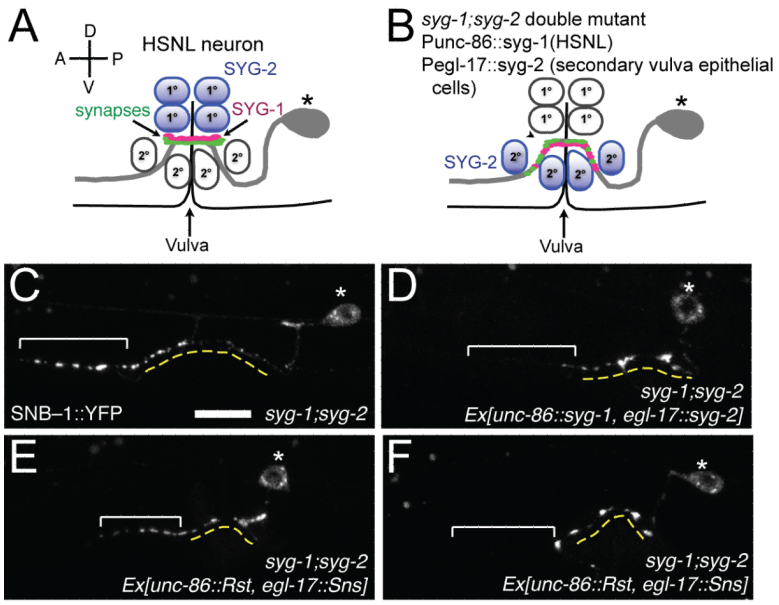

Figure 6. SYG-1 and SYG-2 D1s can be replaced with orthologous domains to partially rescue the *syg-1;syg-2* double mutant defects

A. Schematic representation of HSNL synapses at the vulva in wild-type worms, in which SYG-2 is expressed in primary vulval epithelial cells.

B. Schematic representation of HSNL synapses at the vulva in *syg-1;syg-2* double mutant worms co-injected with *syg-1* under the control of *unc-86* promoter, and *syg-2* under the control of *egl-17* promoter. Since *egl-17* promoter drives *syg-2* expression in secondary vulval epithelial cells, a wider region for synaptic vesicle clustering is observed.

C.*syg-1;syg-2* worms show synaptic vesicles in the ectopic anterior region. The dashed yellow line denotes the extent of the secondary cells. The bracket highlights ectopic clustering of SNB-1 in the anterior axon.

D. Co-injection of *syg-1;syg-2* animalswith *Punc86::syg-1* and *Pegl-17::syg-2* results in clustering of synaptic vesicles around the vulva, as explained in (B).Injection of *syg-1* alone fails to rescue the synapses in the *syg-1;syg-2* mutant (Figure 6A).

E-F. Co-injection of *syg-1* whereits D1 is replaced with D1 of Rst and *syg-2* where its D1 is replaced with D1 of SNS rescues synaptic defects in some animals (F), but not in others (E). Rescue in (F) resembles that in (D).

See also Figure S6.

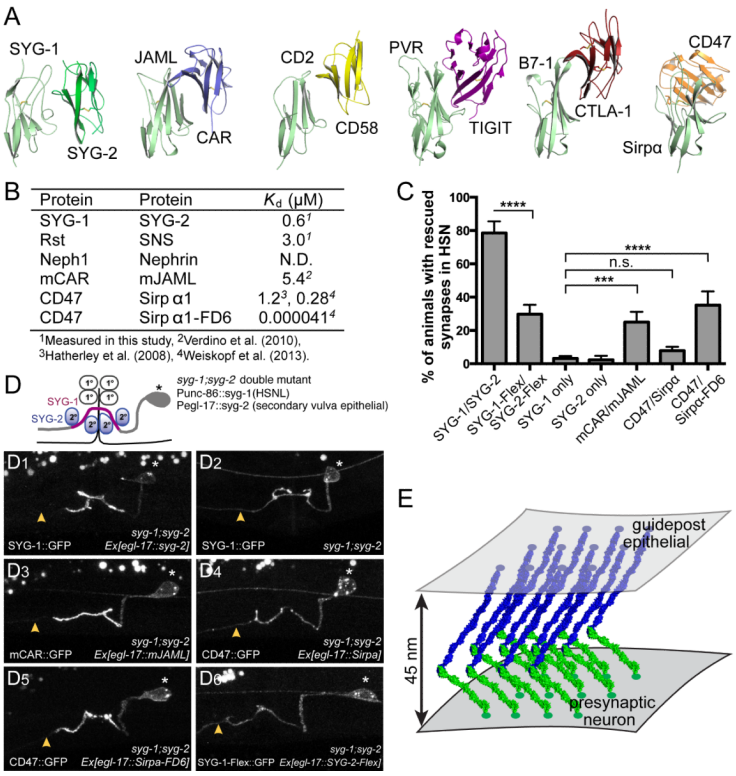

Figure 7. Rescue efficiency of *syg-1;syg-2* double mutant defects depends on the approach geometry and rigidity of the interacting ectodomains

A. Comparison of SYG-1/SYG-2 with known structures of Ig-CAM hetero-complexes, all mediated through D1 domains. The structures are ordered from left to right in terms of decreasing similarity to SYG-1/SYG-2 with regards to the approach geometry, where the mouse JAML/CAR complex is most similar,and the CD47/Sirpα complex is most different to the SYG-1/SYG-2 complex.

B. A guide to affinities between the studied complexes as dissociation constants (in μM).

C. Quantitation of rescue (as phenotype scores) of *syg-1;syg-2* worms when D1s are replaced by D1 domains from indicated proteins. ***p< 0.001; **** p< 0.0001;n.s., not significant.CAR/JAML D1s can partially rescue *syg-1;syg-2*, but the geometrically different CD47/Sirpα cannot. Lack of CD47/Sirpα can be, however, ameliorated when an extremely high-affinity variant of Sirpα (FD6) is used. Also included is rescue with SYG-1 and SYG-2 modified with flexible interdomain linkers (SYG-1-Flex/SYG-2-Flex), which is significantly diminished compared to rigid WT SYG-1/SYG-2.

D.Representative images of the localization of SYG-1 chimeras and the flexible SYG-1 variant. For chimeras, SYG-1 D1 domains were replaced with those from other Ig domains involved in Ig-CAM interactions. SYG-1 constructs have been tagged with a C-terminal GFP and expressed in *syg-1 syg-2* double mutant background together with the corresponding untagged SYG-2 chimera binding partner in the secondary vulva epithelial cells.

(D1) Enrichment of WT SYG-1::GFP to the axonal regions in contact with SYG-2 expressing secondary vulva epithelial cell. The axon segment anterior to the synaptic region is devoid of SYG-1::GFP staining as denoted by yellow arrow.

(D2) SYG-1::GFP expression alone without SYG-2 is diffusely localized along the entire axon.

(D3) mCAR-SYG-1::GFP and mJAML-SYG-2 which has similar approach geometry as SYG-1 and SYG-2 shows proper localization and enrichment suggestive of binding.

(D4) CD47-SYG-1::GFP and Sirpa-SYG-2 with dissimilar approach geometry fails to localize and is found diffused along the entire axon.
(D5) Sirpa-FD6-SYG-2 which has very high affinity for CD47::GFP results in the subcellular enrichment of CD47::GFP.
(D6) Flexible SYG-1 (SYG-1-Flex::GFP) is found diffused along the entire axon, indicative of proper expression and targeting to the membrane, but is not enriched where SYG-2-Flex is expressed.
E. Suggested cellular adhesion model involving SYG-1 (green), SYG-2 (blue).